

An Approach to Inline Monitoring of the Electrode State in Resistance Spot Welding

Samiha Durnagöz^{1,2,3,*}, Marco F. Huber^{3,4}, Mathias Mayer⁵, and Peter Reimann^{1,6}

¹ Graduate School of Excellence Advanced Manufacturing Engineering, University of Stuttgart, Stuttgart, Germany

² AUDI AG, Neckarsulm, Germany

³ Institute of Industrial Manufacturing and Management IFF, University of Stuttgart, Stuttgart, Germany

⁴ Fraunhofer Institute for Manufacturing Engineering and Automation IPA, Stuttgart, Germany

⁵ Innovation Management, Production Lab, AUDI AG, Neckarsulm, Germany

⁶ Institute for Parallel and Distributed Systems IPVS, University of Stuttgart, Stuttgart, Germany

Email: Samiha.Durnagoetz@gsame.uni-stuttgart.de (S.D.), Marco.Huber@ieee.org (M.F.H.),

Mathias.Mayer@audi.de (M.M.), Peter.Reimann@gsame.uni-stuttgart.de (P.R.)

Abstract—Resistance Spot Welding (RSW) is a key technology for joining car body parts. During the process, the upper and lower electrodes of the welding gun are subject to wear, which affects the electric current flow and thus, the quality of the spot weld. To counteract this effect, the electrode tip is dressed after a predefined number of spot welds. The frequency for tip dressing is based on experience and does currently not directly reflect the actual state of the electrode. This work provides an approach to inline electrode state monitoring to determine the ideal and demand-based point in time for electrode tip dressing based on process data. We avoid costly and time-intensive experimental labeling of electrode states and utilize changes in the dynamic electrical resistance between dressing cycles to represent the electrode wear state. To describe the changes in the dynamic electrical resistance curve, new features such as the peak time delay are calculated and visualized. We evaluate our approach with a real-world data set that stems from a dynamic and complex environment out of a series production line, which, in contrast to laboratory data, ensures a successful application of the proposed methods in an industrial setting.

Index Terms—industrial data analytics, resistance spot welding, electrode wear state monitoring, feature construction, data mining

I. INTRODUCTION

Resistance spot welding (RSW) is a key joining technology in automotive manufacturing and is characterized by a high degree of automation and robotization [1]. In a typical body shop, several hundred industrial robots produce over 5,000 spot welds per vehicle. During the RSW process, two or more overlapping metal sheets are clamped together by a welding gun, and an electric current is induced through the electrodes [2]. The generated electric circuit produces an electrical resistance between the work pieces, and the obtained heat results in local melting, thus forming a coalescence [2].

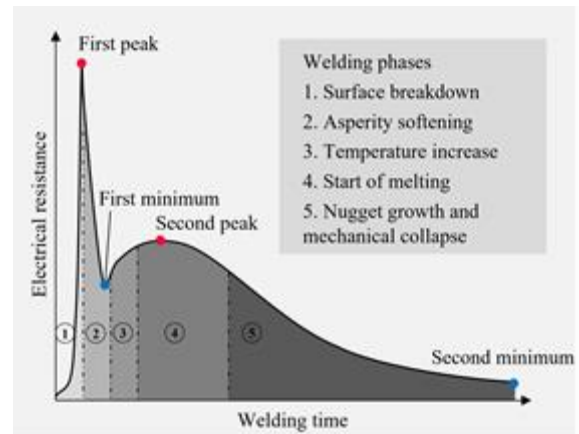


Fig. 1. A typical DERC with five welding phases according to Dickinson *et al.* [3] and stationary points.

A typical dynamic electrical resistance curve (DERC) is given in Fig. 1, where five welding phases can be described according to Dickinson *et al.* [3]. In the first phases, the applied force and an initial generation of heat break down surface contaminants, e.g., adhesive residue. This results in an initial sharp electrical resistance drop in the second welding phase. The contact area of the metals increases, and the first resistance minimum is reached. This is due to the softening of asperities, i.e., high spots on the sheet metal's surface. In the fourth phase, the electrical resistance increases and melting starts. A second resistance peak is reached, and the temperature begins to stabilize while the weld nugget, which is formed from molten material, grows and mechanical collapse starts to dominate. This results in a decrease in the electrical resistance in the fifth phase.

During the welding of galvanized sheet steel, alloying elements of the zinc coating agglomerate on the surface of the electrode tips. Thermal and mechanical loads cause the electrodes to gradually deform, leading to electrode tip growth. This effect is also referred to as mushrooming and impacts the current flow and, as a result, the nugget size and quality of the spot weld [2]. As a consequence, the electrode tip is milled or dressed to its original shape after

a predefined number of spot welds. The shorter the interval for tip dressing, the more cumulated maintenance time is required, leading to frequent production delays to replace worn electrodes. The frequency for tip dressing is based on experience and does not reflect the actual state of the electrode. Furthermore, a generic number for the amount of spot welds between tip dressing is set for several welding machines even though the electrode state is affected by various factors, such as the welding material or the welding equipment, and fluctuates greatly even with the same welding parameters [4, 5]. Therefore, the frequency of tip dressing is chosen in a preventive and pessimistic manner. This results in unused potential and resources for the electrode itself, as well as energy for the subsequent milling of the electrode tip is wasted. Inline condition monitoring of the electrode state enables adaptive and demand-based electrode tip dressing, thus utilizing the missed potentials. The transparency of the RSW process increases, which enables the detection of abnormal behavior. This provides the foundation for a feedback control system to avoid the manufacturing of spot welds that do not meet the required quality.

Body shops of large automotive manufacturers are characterized by highly automated and complex production environments where up to 3.5 million spot welds are produced daily. The utilization of gradually increasing internet of things (IoT) data enables optimization where conventional methods reach their limitations. Data-based approaches allow non-destructive online monitoring of complex processes and their components [6]. Monitoring the electrode state increases process reliability and stability, and once implemented, the methodology can be transferred to hundreds of industrial robots of a comparable type and even to other use cases and production plants. The applicability of our work enables a feedback control system to produce spot welds that meet the required quality. Our work serves as an example for similar robotized manufacturing processes.

In this work, we propose an approach to inline condition monitoring for the electrode state based on changes in the DERC. We apply, amongst others, methods presented in [5]. In contrast to Zhou *et al.* [5], we apply the methods to real-world process data. The peak time delay in the fourth welding phase and the weighted shape change factor (WSCF) can describe the wear of the electrode state. However, the trend change factor (TCF) and the resistance decrease ratio are fluctuating strongly and a clear trend is not visible. Therefore, we compare the methods presented in [5] to conventional time series similarity methods and generate additional features to describe the electrode state. We show that a combination of carefully selected features can describe the electrode state in real-world process data and that changes in the DERC are visible even over series of 120 spot welds. We apply an unsupervised machine learning (ML) approach that does not require expensive experiments and data labeling. Data mining with real-world process data ensures that our approach is directly applicable in an industrial setting. This enables the deployment and integration of condition monitoring of the electrode state in current processes.

The paper is structured as follows. In the next section, related work on condition monitoring of the electrode state is discussed. In Section III, the data set is introduced. Section IV presents experimental results, where we assess changes in meaningful points in the DERC (Section IV-A), changes considering more features (Section IV-B), and lastly compare all features (Section IV-C). The paper closes with conclusions and an outlook on future work.

II. RELATED WORK

The majority of the research described the electrode state based on changes in the electrode length or the displacement of the electrodes. The results are mainly obtained in an experimental setting and the transferability of the methods to real-world use cases is not ensured. Zhang *et al.* [7] and Zhang *et al.* [8] utilized the positions of servo welding guns to measure the change in the electrode length and detect electrode wear. Mathiszik *et al.* [9] monitored the change in the electrode length over the number of spot welds to determine the electrode wear state. The study showed two wear modes—mushrooming and plateau formation—and determined, among others, the change in the electrode length through the electrode position. In comparison to mushrooming, the plateau is not an agglomeration of alloying elements, but is formed by a consecutive deformation process of the electrode during welding. Wang *et al.* [10] described the electrode wear based on changes in the electrode displacement curves with a moving range method. In [11] the displacement of the electrode tips was directly measured with image sequences of markers on the electrode surface and in [12] the degree of electrode tip wear was predicted with an ML-model based on laser measurements of the electrode tip and digital images of the spot welds. We could not see changes in the length of the electrodes in our data set, and perhaps high-precision laser displacement sensors are required to measure the changes more accurately. The additional cost and complexity of implementing high-precision laser displacement sensors across all plants limit their use. Therefore, our approach is based on changes in the DERC.

In [13], a supervised ML-framework to predict the electrode wear based on multiple sensor measurements and carbon imprints of the electrode tip was proposed. However, to apply the above methods, it is necessary to collect a large amount of data using extensive sensory or even imaging techniques. The integration of additional sensors and equipment into a series production line is expensive, time-consuming, and often complex. The ML approaches require data labeling, which increases costs even further. In comparison, we utilize already existing data, provided by fewer sensors that are already present. This limits the effort and, as a result, allows a real-world application almost immediately.

Takahashi *et al.* [14] developed an automatic voltage determination system to improve the quality and productivity of a resistance welding process. The method utilized real-world process data, where the system learned to react to electrode degradation based on voltage change logs that were generated by experienced operators. Our

focus, however, lies on the determination and monitoring of the electrode state.

Zhou *et al.* [5] proposed a novel online monitoring method of the electrode wear state based on time series similarity and variation patterns of DERCs. The authors reduced the dimensionality of the original DERCs and presented new features to describe the change in the electrode state. According to Zhou *et al.* [5], the electrode state can be divided into three stages: a stable stage, a transition stage, and a deterioration stage. Some presented features, such as the point in time of the second resistance peak fluctuated greatly in the deterioration stage. In contrast to Zhou *et al.* [5], who relied on experimental data, we mine time series similarity changes of the dynamic resistance series in real-world data from a dynamic and complex production environment. This means we treat challenges that accompany mining process data and consider additional influencing factors. The preceding manufacturing steps, e.g., the forming and deep drawing of sheet metal components, can produce inconsistent gaps between the work pieces. Adhesive residue and other surface contaminants can affect the welding quality, and preceding welding operations may result in distortions of the component. Furthermore, with each tip dressing, the cooling channel of the electrode is closer to the contact surface of the electrode. Additionally, we need to consider modifications in the parameters of the adaptive welding controller. The changing conditions can lead to random behavior of the dynamic resistance curve and high variance between curve features. Earlier research did not consider random influencing factors and changing process conditions to this extent. We determine robust features to describe the electrode state, which ensures its applicability in the industry. Moreover, our methods capture change patterns over much shorter intervals, which ensures a fast application to real-world processes. We also juxtapose the presented features against conventional time series similarity methods.

III. DATA SET

The data set contains 11,400 observations, i.e., process information about spot welds and the welding system. The data stem from a series production line where a KUKA KR240 R2900 ULTRA robot equipped with a welding gun repeatedly welds five spot welds along a longitudinal beam of the vehicle body. The materials of the joined body parts are two hot-dipped galvanized steel plates with a thickness of 2.0 and 1.2 mm, respectively. The welding process is performed with a BOS 6000 welding controller from Bosch Rexroth. An optimal DERC is generated in the development phase and serves as a reference to the welding controller. In adaptive mode, the controller aims to map the reference DERC by adjusting the welding parameters. The controller has an internal wear counter variable where each welding process is counted. After 120 spot welds, the electrode tips are dressed, and the counter is set to zero. After 55 dressing intervals, the electrodes are replaced.

For every observation, the data set contains an electric current and voltage curve over the welding time in 1.0 ms

time steps. The welding time ranges from 489 to 655 ms, with a median of 500 ms and 75 % of the observations having a welding time less or equal to 505 ms. The electric current and voltage curves, the deposited reference DERC, and singular features such as welding gun parameters and electrode parameters are passed on via message queuing telemetry transport (MQTT), a messaging protocol used for machine-to-machine communication.

IV. RESULTS AND DISCUSSION

The objective of this work is to apply and propose practical methods to monitor the change in the dynamic resistance between dressing intervals. We derive relationships and coherence between the observed changes and the electrode state. The findings are consistent with previous research results, where in particular the methods of Zhou *et al.* [5] have proven helpful. It can be concluded that the dynamic resistance series changes regularly. The peak resistance in the fourth welding phase (second resistance peak in Fig. 1) decreases gradually, and the corresponding point in time increases with a rising number of spot welds. This is mainly due to the electrode tip diameter gradually growing and the current density gradually decreasing. As a result, the rising speed of the dynamic resistance series at the initial stage is gradually reduced, leading to a regular change in the dynamic resistance series (Fig. 2).

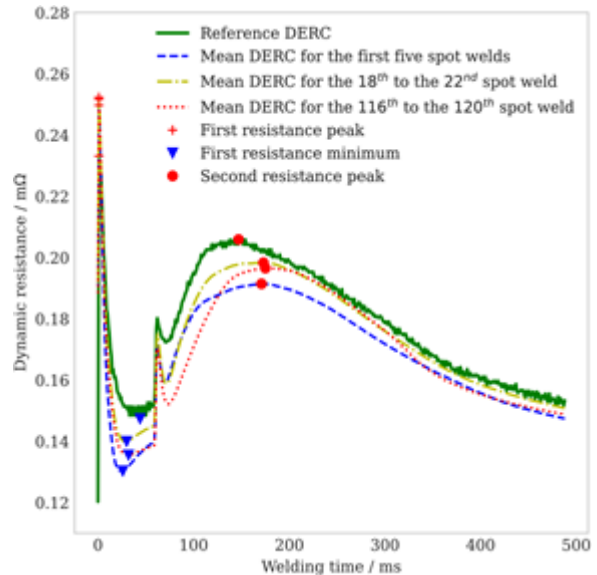


Fig. 2. Comparison between the reference DERC, the mean DERC for the first five spot welds, the mean DERC for the 18th to the 22nd spot weld, and the mean DERC for the 116th to the 120th spot weld.

A typical DERC consists of around 500 measured resistance values. To reduce computational costs and neglect non-meaningful information, the dimension of the DERC is reduced in two manners. In the first approach, only meaningful points such as the first resistance minimum and second resistance peak and their corresponding points in time are calculated, and the rest of the curve is neglected (Section IV-A). The second approach regards more points of the DERC (Section IV-B). We calculate the dynamic electrical resistance decrease

ratio and the TCF and WSCF according to Zhou *et al.* [5]. Furthermore, we compare the features to conventional time series similarity methods, such as the Dynamic Time Warping Distance (DTWD), the trapezoidal area under the resistance curve, and the Fréchet distance.

We aim to find robust features to describe the electrode state and show a clear trend over the number of spot welds. The objective is to derive relationships and coherence between the observed changes and the progressing electrode degradation. Computational costs should be kept to a minimum, without missing meaningful information. We show that the WSCF, the change in meaningful points of the DERC, and the DTWD are suited to describe the electrode wear state (Section IV-C). With the application to real-world process data we consider additional influencing factors and ensure that our methods can be applied in an industrial setting for inline condition monitoring of the electrode state.

A. Changes in Meaningful Points in the DERC

In the first approach, we determine stationary points in the DERC. Fig. 2 shows mean DERCs with their stationary points over different welding numbers. The first resistance minimum and the second resistance peak, as well as their corresponding points in time are calculated.

In Fig. 3, the point in time of the second resistance peak is depicted over all 120 spot welds. The resistance series shows a periodic pattern of change over the five positions of the spot welds along the component. Therefore, the moving average with a window size of five is calculated to visualize the trend over all 120 spot welds. Since the moving variance decreases with an increasing amount of spot welds, we can assume that the welding is still in a stable stage and the electrode is not yet worn. This indicates that the tip dressing interval can be increased. The delay of the point in time of the second resistance peak is valid for each of the five positions of the spot welds along the component.

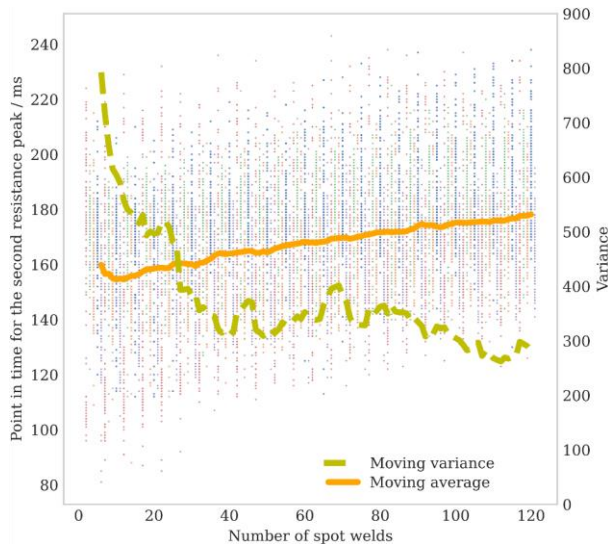


Fig. 3. Point in time of the second resistance peak in the fourth welding phase. Depicted for all five positions of the spot welds along the component over the dressing interval.

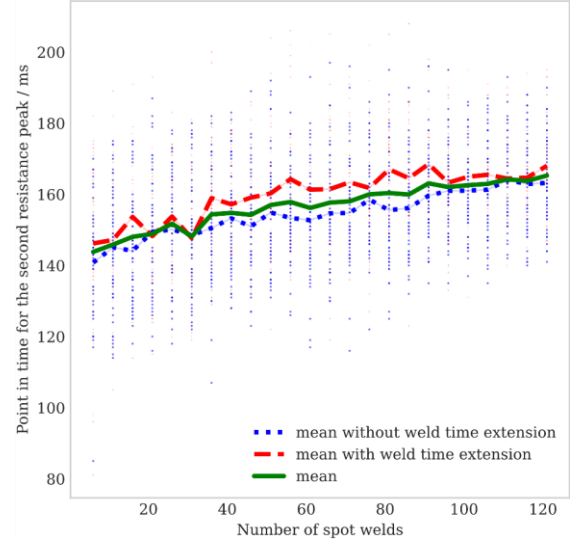


Fig. 4. Mean values for points in time of the second resistance peak of spot welds with and without weld time extensions, and the mean values of all spot welds. Only one welding position on the component is depicted over the dressing interval.

In Fig. 4, the point in time of the second resistance peak over all 120 spot welds is depicted for one of the five spot weld positions, and the same pattern can be observed. This is also valid for DERCs, where a weld time extension is assigned automatically by the adaptive mode of the welding controller.

Our results coincide with the findings of [5] and a mean time delay of 17.5 ms of the second resistance peak can be observed towards the end of the interval compared to the reference DERC. The moving variance drops from 792.6 to 282.2 towards the last spot welds. Zhou *et al.* [5] showed that the point in time of the second resistance peak fluctuates greatly when the influence of random factors such as contact surface alloying and surface pitting, where material is removed from the electrode tip face, begins. Therefore, we can safely assume that the electrode state is still in a stable phase.

To compare further features, we calculate the moving average with a window size of five over all 120 spot welds and apply the standard scaler by means of the Python package scikit-learn. In Fig. 5, further features regarding a singular point in the resistance curve are shown. We analyze the value of the first resistance minimum and the point in time of the first resistance minimum, and the value of the second resistance peak. The dynamic resistance values at the first resistance minimum and second resistance peak are increasing at first. The resistance values at the first resistance minimum are starting to decrease after the 22nd welding procedure. The resistance values of the second resistance peak start to decrease after the 51th welding procedure. Both values then decrease until the end of the interval at 120 spot welds. The corresponding time values are increasing continuously. It can be assumed that the first resistance minimum and corresponding time are influenced by random conditions like surface contaminants and the distance between the components, leading to higher fluctuations. Therefore, the second resistance peak and the point in time of the second

resistance peak are more suitable for condition monitoring. Here, random surface contaminants are already broken down, and the softened asperities result in increasing metal-to-metal contact, causing a steady current flow.

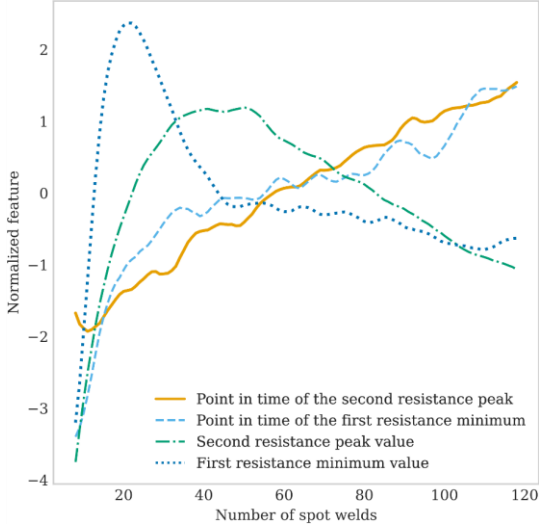


Fig. 5. Moving average for normalized features (second resistance peak and point in time of the second resistance peak, first resistance minimum and point in time of the first resistance minimum) over the number of spot welds.

B. Changes in the DERC Considering More Features

Describing the changes in the DERC with only one point with two values may result in the loss of a significant amount of information. Therefore, further features are calculated based on a lower dimension of the DERC. We examine the resistance decrease ratio, which describes the ratio between the peak in the fourth welding phase and the resistance end value, the WSCF, and the TCF according to Zhou *et al.* [5]. Additionally, we compare our results to methods considering the whole resistance curve, where we apply trapezoidal numerical integration to calculate the area under the resistance curve. We further calculate the Fréchet distance and the DTWD between resistance curves.

The WSCF describes a weighted Euclidean distance between reduced representations (in our case, 18 equally spaced points between a welding time of 0 and 487 Milliseconds in 27 Milliseconds time steps) of the DERC and the reference DERC and is defined according to Zhou *et al.* [5] as

$$\text{WSCF}(r^k, r^{\text{ref}}) := \sqrt{\sum_{i=1}^{18} w_i \cdot (r_i^k - r_i^{\text{ref}})^2},$$

where $r^k = (r_1^k, \dots, r_{18}^k)$, $r^{\text{ref}} = (r_1^{\text{ref}}, \dots, r_{18}^{\text{ref}})$ represent the 18 points of the two curves, and

$$w_i := \left(1 + \exp\left(-\frac{i-2}{4}\right)\right)^{-1}$$

is the gradually increasing weight; thus, a greater focus is laid on the end of the reduced DERC. To remove noise, we apply the Savgol filter and normalize the DERC with the Z-score normalization method before reducing the curve

to 18 resistance and time values. In contrast to Zhou *et al.* [5], we calculate the WSCF between the reference DERC and the dynamic resistance series over 120 spot welds. Fig. 6 shows the scattered mean values of the WSCF over the number of spot welds and the moving average over a window size of five. The WSCF fluctuates stronger in the initial stage with a value of 1.6 and, after reaching a local minimum of 1.4 at the 15th spot weld, gradually increases over the number of spot welds. A maximum of 1.77 is reached at the 120th spot weld.

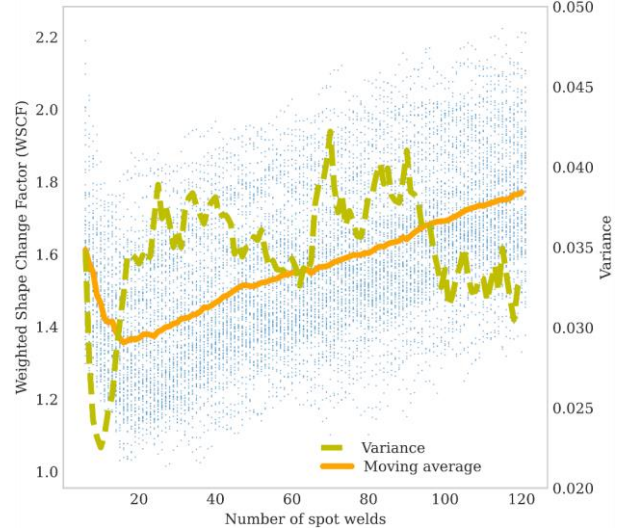


Fig. 6. The mean WSCF over all 120 spot welds with the moving average and the moving variance.

We compare the WSCF to further features calculated with more than a single point of the resistance curve. The normalized moving averages of some of the generated features are visualized in Fig. 7. We compare the WSCF, the TCF, the resistance decrease ratio, the trapezoidal area under the resistance curve, the Fréchet distance and the DTWD to the reference curve. The WSCF and the DTWD show a clear trend over all 120 spot welds, whereas the other higher dimensional features fluctuate greatly, and the changing process of the electrode state is therefore not clear.

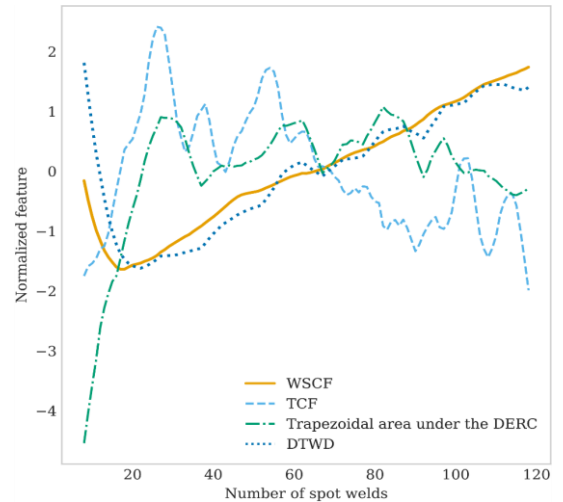


Fig. 7. Moving average for normalized higher dimensional curve features (WSCF, TCF, trapezoidal area under the DERC and the DTWD) over the number of spot welds.

C. Comparison of All Features

Our analysis reveals that the WSCF, the DTWD, the second resistance peak, and the point in time of the second resistance peak are suitable to describe the electrode state. The second resistance peak increases until the 51st spot weld and then decreases towards the end of the interval without significant fluctuations. The point in time of the second resistance peak reaches a minimum at the 12th spot weld and then increases gradually over the number of spot welds. The WSCF reaches a minimum at the 18th spot weld and gradually increases over the number of spot welds without significant fluctuations. Similar characteristics can be observed for the DTWD. In contrast, the TCF, the Fréchet distance, the resistance decrease ratio or the trapezoidal area under the resistance curve fluctuate significantly and a clear trend over the number of spot welds is not visible. Therefore, these features are not suitable for condition monitoring of the electrode state in the presented use case.

Our findings regarding the delay in the point in time of the second resistance peak and the behavior of the WSCF are in agreement with Zhou *et al.* [5], who showed that these features are appropriate to monitor the electrode state.

The second resistance peak carries meaningful information about the welding quality. Hence, it is necessary to include the feature in condition monitoring. We find that conventional time series similarity methods, such as the DTWD, show good results and, by considering all points of the DERC, we ensure that no information is missed. In case computational costs and latency are secondary requirements, the DTWD can be included in condition monitoring.

Our findings enable domain experts to define thresholds at which tip dressing is required. Due to the position of the spot weld and random noise, feature values still fluctuate between subsequent spot welds. Therefore, thresholds for the moving average of the feature values are generally better suited to define the point in time for tip dressing.

V. CONCLUSION AND FUTURE WORK

The RSW process is characterized by complex behavior, and patterns in the data are difficult to detect. Noise and random effects in the DERC hamper the monitoring of the electrode wear state. Additionally, in real-world process data, the configurations of the welding controller, such as the weld time extension, must also be considered. We assess the wear state of the electrodes indirectly by mining dynamic resistance data. We show that the proposed methods are suitable for monitoring the electrode wear state in an industrial setting. The electrode wear process can be visualized by calculating the similarity of the dynamic resistance series between subsequent welding points and the reference resistance curve. Based on the analysis of our methods and comparison to the findings of Zhou *et al.* [5], the change in the electrode state in this study is still in a stable phase. This indicates the unused potential of the electrodes and would allow further welding.

Future work will concentrate on the application of the methods to further welding robots, where more complex components and a higher variety of component types are

welded. Our work also forms the basis for a feedback control system to manufacture spot welds that meet the required quality. In case an abnormal behavior in the electrode state is detected, the feedback control system can prevent loss in quality, for instance, through the timely initiation of the tip dressing process. Since the robots and control units are of comparable type, the feedback control system can be transferred to several hundred industrial robots in the same production line and even to other production plants. We will also focus on describing the remaining variance between subsequent spot welds to establish a more robust solution for electrode condition monitoring.

CONFLICT OF INTEREST

The authors declare no conflict of interest.

AUTHOR CONTRIBUTIONS

Samiha Durnagöz conducted the research and wrote the paper; Mathias Mayer provided the data set; Prof. Marco Huber and Peter Reimann revised the paper and provided scientific advisory; all authors had approved the final version.

ACKNOWLEDGMENT

This work was supported by the Ministry of Science, Research and the Arts of the State of Baden-Württemberg within the sustainability support of the projects of the Excellence Initiative II.

REFERENCES

- [1] N. Williams and J. Parker, "Review of resistance spot welding of steel sheets part 1 modelling and control of weld nugget formation," *International Materials Reviews*, vol. 49, no. 2, pp. 45-75, 2004.
- [2] H. B. Cary, *Modern Welding Technology*, 2nd ed. Prentice-Hall, Inc., 1988.
- [3] Dickinson, D. W., J. E. Franklin, and A. Stanya, "Characterization of spot welding behavior by dynamic electrical parameter monitoring," *Welding Journal*, vol. 59, no. 6, p. 170, 1980.
- [4] S. Fukumoto, I. Lum, E. Biro, D. Boomer, Y. Zhou *et al.*, "Effects of electrode degradation on electrode life in resistance spot welding of aluminum alloy 5182," *Welding Journal*, vol. 82, no. 11, pp. 307-310, 2003.
- [5] L. Zhou, T. Li, W. Zheng, Z. Zhang, Z. Lei, L. Wu, S. Zhu, and W. Wang, "Online monitoring of resistance spot welding electrode wear state based on dynamic resistance," *Journal of Intelligent Manufacturing*, vol. 33, pp. 91-101, 2022.
- [6] B. Zhou, "Machine learning methods for product quality monitoring in electric resistance welding," Ph.D. dissertation, Karlsruhe Institute of Technology, Karlsruhe, GE, April 2021.
- [7] Y. Zhang, H. Wang, G. Chen, and X. Zhang, "Monitoring and intelligent control of electrode wear based on a measured electrode displacement curve in resistance spot welding," *Measurement Science and Technology*, vol. 18, no. 3, p. 867, 2007.
- [8] X. Zhang, G. Chen, and Y. Zhang, "On-line evaluation of electrode wear by servo gun in resistance spot welding," *The International Journal of Advanced Manufacturing Technology*, vol. 36, pp. 681-688, 2008.
- [9] C. Mathiszik, D. Küberlin, S. Heilmann, J. Zschetzschke, and U. Füssel, "General approach for inline electrode wear monitoring at resistance spot welding," *Processes*, vol. 9, no. 4, p. 685, 2021.
- [10] H. Wang, Y. Zhang, and G. Chen, "Resistance spot welding processing monitoring based on electrode displacement curve using moving range chart," *Measurement*, vol. 42, no. 7, pp. 1032-1038, 2009.
- [11] L. Kuščer, I. Polajnar, and J. Diaci, "A method for measuring

displacement and deformation of electrodes during resistance spot welding,” *Measurement Science and Technology*, vol. 22, no. 6, p. 067002, 2011.

- [12] J. Zhang, P. X. Zhang, and X. J. Xu, “A model for predicting the wear degree of electrode tip,” *Applied Mechanics and Materials*, vol. 574, pp. 292–297, 2014.
- [13] L. Panza, G. Bruno, M. De Maddis, F. Lombardi, P. R. Spena, and E. Traini, “Data-driven framework for electrode wear prediction in resistance spot welding,” in *Proc. IFIP International Conference on Product Lifecycle Management*, Curitiba, Brazil, 2021, pp. 239–252.
- [14] M. Takahashi, T. Yasui, and K. Muro, “Domain knowledge-based automatic voltage determination system for welding machine,” *International Journal of Electrical and Electronic Engineering & Telecommunications*, vol. 10, no. 4, pp. 294–299, 2021.

Copyright © 2024 by the authors. This is an open access article distributed under the Creative Commons Attribution License (CC BY-NC-ND 4.0), which permits use, distribution and reproduction in any medium, provided that the article is properly cited, the use is non-commercial and no modifications or adaptations are made.



Samiha Durnagöz received a BSc and MSc degree in Mechanical Engineering from the Friedrich-Alexander-University of Erlangen-Nuremberg. She currently is a Ph.D. student at the University of Stuttgart and the Graduate School of Excellence advanced Manufacturing Engineering (GSaME). Her research, in collaboration with the AUDI AG, focuses on machine learning, data analysis, and data-based process optimization.



Marco Huber received his Ph.D. degree in computer science from the University of Karlsruhe (TH) in 2009. From 2009 to 2011, he headed the research group "Variable Image Extraction and Processing" at the Fraunhofer IOSB in Karlsruhe. He then worked as Senior Research at AGT International in Darmstadt until 2015. From April 2015 to September 2018, Prof. Huber was responsible for product development and data science services of the Katana division at USU Software AG in Karlsruhe. At the same time, he was adjunct professor of computer science with the Karlsruhe Institute of Technology (KIT). Since October 2018, he is professor for cognitive production systems with the University of Stuttgart and he also heads the Center for Cyber-Cognitive Intelligence (CCI) at the Fraunhofer Institute for Manufacturing Engineering and Automation IPA. His research focuses on machine learning, sensor data analysis and robotics for production systems.



Mathias Mayer is a specialist in the Production Laboratory at the AUDI AG. The trained electrical engineer and expert in the field of automation technology has been working at Audi at the Neckarsulm site since 2012. His major research interests include the standardization of Industrial Internet of Things (IIoT), data analysis and the car body shop of the future.



Peter Reimann studied computer science at the University of Stuttgart and received his Ph.D. degree in 2016 at the Institute for Parallel and Distributed Systems (IPVS) and the Cluster of Excellence Simulation Technology (SimTech) at the University of Stuttgart. His Ph.D. topic was related to data management and data provisioning for computer-based simulations and simulation workflows. From July to September 2015, he was a visiting scholar at the School of Information Sciences (iSchool) and the National Center for Supercomputing Applications (NCSA) at the University of Illinois at Urbana-Champaign in the USA. Since 2017, he is a head of a junior research group at the Graduate School of Excellence advanced Manufacturing Engineering (GSaME) at the University of Stuttgart. His current research area covers topics on both application-oriented and fundamental research in the areas of data provisioning, data management, data analysis, and machine learning for industrial use cases (Industrial Analytics).